FUDMA Journal of Sciences (FJS)
ISSN online: 2616-1370
ISSN print: 2645 - 2944
Vol. 10 No. 23, December, 2026, pp 236 – 245
DOI: https://doi.org/10.33003/fjs-2026-1023-6230

Response Surface Methodology-Based Modelling, Optimization and Validation of Sustainable Concrete Incorporating Waste Ceramic Tile Powder and Rice Husk Fibres

[*1]Adefila Abudllahi Ayodeji, [2]Okorie Austine Uche, [3]Nurudeen Yusuf

[1]Department of Civil Engineering, Nigerian Defence Academy, Kaduna, Nigeria
[2]Department of Civil Engineering, Bayero University Kano, Nigeria
[3]Department of Civil Engineering, Usmanu Dan Fodiyo University Sokoto, Nigeria

*Corresponding authors' email: engradefilaaa@gmail.com Phone: +234803-047-5734

ABSTRACT
This study developed, optimized and experimentally validated Response Surface Methodology (RSM) models for concrete containing waste ceramic tile powder (WCTP) and rice husk fibre (RHF). An I-optimal mixture–process design generated with Design-Expert Version 13 comprised 19 runs representing 14 unique formulations and five repeated design points. WCTP replaced Portland Limestone Cement (PLC) over 0–30% of the 425 kg/m³ cementitious content, while RHF was varied from 0–2% by concrete volume (approximately 0–20.4 kg/m³). RSM models were fitted to the 28-day responses for water absorption, sulphate resistance, ambient compressive strength, and residual compressive strength after exposure to 718°C for 15 min and 821°C for 30 min. All models were significant ($p < 0.0001$), with R^2 values of 0.9707–0.9906 and nonsignificant lack-of-fit tests ($p = 0.0561$–0.6994). Numerical optimization produced a mixture of 10.5% WCTP, 89.5% PLC and 0.03% RHF by volume (approximately 0.31 kg/m³), with an overall desirability of 0.745. The predicted responses were 2.85% water absorption, 7.29 N/mm^2 sulphate resistance, 33.71 N/mm^2 ambient compressive strength, and 29.72 and 27.72 N/mm^2 residual strength at 718°C and 821°C, respectively. Experimental validation gave 2.72%, 7.00, 32.18, 28.35 and 26.56 N/mm^2, respectively, with relative prediction errors of 4.14–4.83%. The measured ambient strength of the optimized mixture was 5.4% lower than the 34.0 N/mm^2 control at 28 days, showing that the optimum represents a multi-response compromise rather than the maximum-strength formulation. The models are therefore useful for prediction within the investigated design domain, subject to further validation.

Received: 11 Sept. 2026
Accepted: 13 Nov. 2026
Published: 16 Nov. 2026

Keywords: Polyherbal Formulation, Antidiabetic, Syrup, LD50, GC-MS, Diabetes Mellitus

INTRODUCTION

Concrete remains indispensable to infrastructure development, but its production is associated with substantial environmental burdens, particularly those linked to cement manufacture and the extraction of natural resources. Partial replacement of cement with waste-derived supplementary cementitious materials is therefore an important route to reducing clinker demand while maintaining useful engineering performance (Scrivener et al., 2018; International Energy Agency, 2023).

Waste ceramic tile powder (WCTP) is attractive because finely ground ceramic waste contains substantial silica and alumina and can contribute to secondary cementitious reactions. Previous studies have reported improvements in selected strength and durability properties when ceramic waste is used at controlled replacement levels (Medina et al., 2013; Singh & Siddique, 2017; Siddique et al., 2023). The response, however, is not necessarily linear because increasing ceramic replacement also reduces the amount of Portland cement available for primary hydration.

Rice husk fibre (RHF) represents a different type of waste-derived material. In the present study, RHF refers to processed rice husk used as a discrete lignocellulosic reinforcement; it is not untreated rice husk and it is not rice husk ash. Unlike rice husk ash, which is produced by combustion and is normally considered an ash-based supplementary cementitious material, RHF is retained as a fibrous reinforcement. Its potential role is therefore associated with crack bridging, stress transfer and modification of composite microstructure rather than primarily with pozzolanic activity (Bisht & Ramana, 2020; Kumar & Bhattacharyya, 2021; Onuaguluchi & Banthia, 2022).

The fibre used in this study was alkali treated before incorporation. Its measured average length of 7.2 mm, diameter of 0.3 mm and aspect ratio of 24 indicate a geometry capable of contributing to crack restraint, while its tensile strength of 120 N/mm^2 supports its use as reinforcement. At the same time, the high water absorption of lignocellulosic fibre can alter water demand, workability and matrix continuity as dosage increases (Chen et al., 2021; Kumar & Bhattacharyya, 2021).

The literature also shows that ceramic-powder concrete and natural-fibre concrete have often been studied separately or with emphasis on individual responses. Medina et al. (2013) and Singh and Siddique (2017) examined ceramic waste as a cementitious component, whereas Bisht and Ramana (2020) focused on discarded rice husk fibre. Tayeh et al. (2021) also investigated hybrid waste ceramic–agricultural fibre systems, while Adamu et al. (2022) and Hadee & Shakeel (2022) applied RSM to concrete mix optimization and ceramic-powder systems. What remains less clear is how WCTP and RHF interact when moisture absorption, sulphate exposure response, ambient strength and post-fire residual strength are considered together.

The novelty of the present work therefore lies in the materials-performance question rather than in the use of Optimal Custom Design alone: can a constrained WCTP–

PLC binder system combined with a separate RHF process variable be modelled sufficiently well to identify a practical compromise among durability, ambient strength and residual strength after severe thermal exposure? RSM provides the analytical framework to answer that question, while the experimental data support the trade-off assessment (Montgomery, 2019; Myers et al., 2016; Scheffé, 1958).

The aim was to develop, optimize and validate predictive models for WCTP–RHF concrete. The study quantified the effects of WCTP and RHF on water absorption, sulphate resistance, ambient compressive strength and residual compressive strength after 718°C and 821°C exposure; evaluated model significance and adequacy; identified a multi-response optimum; and verified the optimum experimentally.

MATERIALS AND METHODS

Materials and Material Preparation

Portland Limestone Cement (PLC), strength class 42.5 N, manufactured by Dangote Cement Plc and procured from a building-materials supplier in Mando, Kaduna State, Nigeria, was used as the primary binder. Waste ceramic tiles were collected from construction and demolition sites within Kaduna State, cleaned, crushed with a jaw crusher, ground in a ball mill and sieved to obtain powder passing 75 µm. Rice husk was obtained from rice milling activities at Station Market, Kaduna South Local Government Area. The husk was cleaned, processed into fibre and immersed in 1% NaOH solution for 24 h at 25 ± 2°C; the treated fibre was rinsed with potable water and air-dried for 48 h before mixing.

The WCTP had a specific gravity of 2.15 and approximately 92% of its particles passed the 75 µm sieve. XRF analysis gave 69.54% SiO_2, 9.60% Al_2O_3 and 2.77% Fe_2O_3, giving a combined $SiO_2 + Al_2O_3 + Fe_2O_3$ content of 81.91%. The RHF had an average length of 7.2 mm, diameter of 0.3 mm, aspect ratio of 24, density of 1,020 kg/m³, tensile strength of 120 N/mm2 and water absorption of 135%. Fine aggregate was natural river sand from the Bugai River in Chikun LGA, while coarse aggregate was crushed granite with a nominal maximum size of 19 mm. Potable water from the Civil Engineering Laboratory of the Nigerian Defence Academy was used for mixing, treatment and curing.

Table 1: Principal Materials and Characteristics

Material	Use/basis	Key characteristics
Portland Limestone Cement	42.5 N	Specific gravity 3.15; bulk density 1440 kg/m³
Waste ceramic tile powder	0–30% of cementitious binder	Specific gravity 2.15; 92% passing 75 µm; $SiO_2+Al_2O_3+Fe_2O_3$ = 81.91%
Rice husk fibre	0–2% v/v concrete	Length 7.2 mm; diameter 0.3 mm; aspect ratio 24; density 1020 kg/m³; tensile strength 120 N/mm2
Fine aggregate	660 kg/m³	River sand; specific gravity 2.61; absorption 0.89%; fineness modulus 2.57
Coarse aggregate	1097 kg/m³	Crushed granite; specific gravity 2.69; absorption 0.70%
Water	190 kg/m³	Potable laboratory water

Mix Proportioning and Definition of Variables

The base concrete was proportioned for an M30 target using a total cementitious content of 425 kg/m³ and a water-to-cementitious-material ratio of 0.45. The fixed quantities of fine aggregate, coarse aggregate and water were 660, 1097 and 190 kg/m³, respectively. WCTP and PLC were treated as constrained mixture components such that WCTP + PLC = 100% of the cementitious binder. RHF was treated separately as a process variable and specified by volume of concrete from 0 to 2% v/v. Using the measured RHF density of 1,020 kg/m³, this corresponds to approximately 0–20.4 kg/m³; the optimized 0.03% v/v corresponds to approximately 0.31 kg/m³.

Table 2: Base Mix Quantities and Variable Definitions

Parameter	Value/range	Unit or basis
Total cementitious material	425	kg/m³
Water	190	kg/m³
Water-to-cementitious-material ratio	0.45	–
Fine aggregate	660	kg/m³
Coarse aggregate	1097	kg/m³
WCTP	0–30	% of cementitious binder
PLC	70–100	% of cementitious binder
RHF	0–2	% v/v of concrete (≈0–20.4 kg/m³)

Experimental Design

An Optimal Custom Design was generated in Design-Expert Version 13 using an I-optimal point-exchange algorithm. The design comprised 19 runs representing 14 unique formulations, with five repeated design points. This structure reflects the constrained mixture–process formulation: WCTP and PLC are not freely independent because their percentages sum to 100%, whereas RHF varies independently as a separate process variable.

The source project records report formulation-level mean responses. Three specimens were used for each mix and curing age for the principal hardened-concrete tests, but individual specimen-level readings were not retained in the source material used for this revision. Accordingly, the revised manuscript does not invent specimen-level standard deviations or error bars; model-level standard deviation and coefficient of variation are reported instead.

Table 3: Complete 19-Run Design Matrix and 28-Day Response Data

Run	WCTP %	PLC %	RHF % v/v	WCTP kg/m³	PLC kg/m³	RHF kg/m³	WA %	SR N/mm²	Fc20 N/mm²	TR718 N/mm²	TR821 N/mm²
1	7	93	0	29.75	395.25	0.000	2.67	7.6	36	31.7	29.5
2	30	70	0	127.50	297.50	0.000	4.82	9.6	20	18	18.3
3	0	100	0	0.00	425.00	0.000	3.62	8.8	34	30.1	27.6
4	22	78	1.5	93.50	331.50	15.300	4.5	9.7	18.6	16	14.2
5	15	85	2	63.75	361.25	20.400	3.77	9.2	23	20.4	18
6	30	70	1	127.50	297.50	10.200	4.77	9.88	21	16.95	15.25
7	15	85	1	63.75	361.25	10.200	3.46	8.4	26	23	20.53
8	7	93	0.5	29.75	395.25	5.100	2.9	7.8	33	29.4	27.2
9	30	70	1	127.50	297.50	10.200	4.77	9.88	21	16.95	15.25
10	0	100	0	0.00	425.00	0.000	3.62	8.8	34	30.1	27.6
11	7	93	1.5	29.75	395.25	15.300	2.84	8.3	29	26.8	24.2
12	0	100	2	0.00	425.00	20.400	3.92	9.5	27	24.6	21.9
13	15	85	2	63.75	361.25	20.400	3.77	9.2	23	20.4	18
14	15	85	1	63.75	361.25	10.200	3.46	8.4	26	23	20.53
15	15	85	1	63.75	361.25	10.200	3.46	8.4	26	23	20.53
16	30	70	2	127.50	297.50	20.400	4.83	10.33	16	14.2	13.5
17	15	85	0	63.75	361.25	0.000	3.33	6.9	31	27.5	25.8
18	0	100	1	0.00	425.00	10.200	3.75	9.1	32	28.5	25.3
19	22	78	0.5	93.50	331.50	5.100	4.16	8.6	20	17.6	16.5

Mixing, Casting and Curing

Materials were batched by weight using a digital balance with ±0.01 kg accuracy. Coarse aggregate, fine aggregate, PLC and WCTP were dry-mixed for approximately 2 min. The pre-treated RHF was introduced gradually, followed by approximately 80% of the mixing water and 3 min of mixing. The remaining water was then added and mixing continued for a further 2 min. Fresh concrete was placed in cleaned and lightly oiled steel moulds and consolidated on a vibrating table until visible air bubbles had substantially ceased, while avoiding excessive vibration and segregation.

Concrete cubes measuring 100 mm × 100 mm × 100 mm were used for compressive-strength, water-absorption, sulphate-exposure and thermal tests. After casting, the moulds were covered with polyethylene sheets for 24 h, then demoulded and cured in potable water at 23 ± 2°C. Hardened concrete was evaluated at 28, 56 and 90 days; the RSM models in this paper use the 28-day response set.

Test Procedures and Operational Response Definitions

Water absorption was determined using a 24-h immersion procedure based on ASTM C642. Cubes were oven-dried at 105 ± 5°C to constant mass (Wd), immersed in water for 24 h, surface-dried and weighed to obtain the saturated mass (Ws). WA = [(Ws − Wd)/Wd] × 100. Because the complete ASTM C642 sequence was not followed, the measurement is described as 24-h water absorption rather than full ASTM C642 compliance.

Ambient compressive strength was determined on 100-mm cubes using the load-at-failure approach. After 28-day curing, selected cubes were exposed in an electrically controlled muffle furnace to 718°C for 15 min or 821°C for 30 min. Temperature was monitored by the furnace control system. Specimens were allowed to cool naturally in air to room temperature before compression testing. The thermal responses are therefore reported explicitly as residual compressive strength rather than as an undefined thermal-resistance measure.

Statistical Modelling, Diagnostics and Validation

The response variables were modelled using a Cubic × Linear Scheffé mixture–process formulation. A denotes WCTP (%), B denotes PLC (%) and C denotes RHF (% v/v). Because A + B = 100%, A and B are constrained mixture components, whereas C is a separate process variable. The fitted form was:

$$Y = \beta_1 A + \beta_2 B + \beta_3 AB + \beta_4 AC + \beta_5 BC + \beta_6 ABC + \beta_7 AB(A-B) + \beta_8 ABC(A-B)$$

Model adequacy was assessed using ANOVA, R^2, adjusted R^2, predicted R^2, adequate precision (AP), standard deviation, coefficient of variation and lack-of-fit. Diagnostic plots included normal probability, predicted-versus-actual and residual-versus-predicted plots. Individual interaction terms were interpreted from their own p-values rather than from overall model significance alone.

The source project file does not preserve a complete lower-order model-coN/mm2rison table or formal Cook's-distance output. The revised manuscript therefore does not claim that the Cubic × Linear model is statistically superior to every simpler model and does not report unsupported influence statistics. Instead, the retained model is evaluated from its ANOVA, nonsignificant lack-of-fit tests, goodness-of-fit measures and available graphical diagnostics.

Numerical optimization used desirability functions. Water absorption and RHF content were minimized, while sulphate resistance and the three compressive-strength responses were maximized. Because only one independent optimum composition was available for validation, the revised manuscript reports response-specific absolute errors and relative prediction errors rather than pooling MAE and RMSE across responses with different units.

RESULTS AND DISCUSSION

Experimental Response Range at 28 Days

The 28-day responses show clear compositional effects. Water absorption ranged from 2.67% to 4.83%, ambient compressive strength from 16.0 to 36.0 N/mm², residual strength from 14.2 to 31.7 N/mm² at 718°C, and from 13.5 to 29.5 N/mm² at 821°C. The sulphate-resistance response ranged from 6.90 to 10.33 N/mm². The 7% WCTP–93% PLC mixture without RHF produced the highest 28-day ambient and thermal strengths, whereas higher RHF contents generally reduced strength.

These results also show why a single-factor interpretation would be inadequate. The formulation giving the highest

individual strength was not the same as the multi-response optimum identified later. The optimization therefore needs to be read as a compromise among competing responses rather than as a search for the maximum value of one property.

Supplementary Table S1. Full Term-By-Term Anova Results
The Following Tables Reproduce the Complete Anova Output Available in The Project Record for The Five Fitted Responses

Table 4: Water Absorption

Source	Sum of squares	df	Mean square	F-value	p-value	Decision
Model	8.14	7	1.16	165.66	<0.0001	Significant
Linear mixture	4.17	1	4.17	593.8	<0.0001	
AB	2.38	1	2.38	338.92	<0.0001	
AC	0.0001	1	0.0001	0.0126	0.9125	
BC	0.0466	1	0.0466	6.65	0.0257	
ABC	0.0622	1	0.0622	8.86	0.0126	
AB(A−B)	1.09	1	1.09	155.37	<0.0001	
ABC(A−B)	0.023	1	0.023	3.28	0.0973	
Residual	0.0772	11	0.007			
Lack of fit	0.0655	6	0.0109	4.67	0.0561	Not significant
Pure error	0.0117	5	0.0023			
Cor total	8.22	18				

Table 5: Sulphate Resistance

Source	Sum of squares	df	Mean square	F-value	p-value	Decision
Model	13.64	7	1.95	52.14	<0.0001	Significant
Linear mixture	2.79	1	2.79	74.7	<0.0001	
AB	5.33	1	5.33	142.65	<0.0001	
AC	0.2548	1	0.2548	6.82	0.0242	
BC	0.232	1	0.232	6.21	0.03	
ABC	1.05	1	1.05	28.03	0.0003	
AB(A−B)	0.5485	1	0.5485	14.68	0.0028	
ABC(A−B)	0.1638	1	0.1638	4.38	0.0603	
Residual	0.411	11	0.0374			
Lack of fit	0.3046	6	0.0508	2.38	0.1794	Not significant
Pure error	0.1065	5	0.0213			
Cor total	14.05	18				

Table 6: Compressive Strength at 20°C

Source	Sum of squares	df	Mean square	F-value	p-value	Decision
Model	648.77	7	92.68	59.58	<0.0001	Significant
Linear mixture	487.09	1	487.09	313.1	<0.0001	
AB	3.6	1	3.6	2.32	0.1563	
AC	7.65	1	7.65	4.92	0.0485	
BC	23.9	1	23.9	15.36	0.0024	
ABC	1.71	1	1.71	1.1	0.3167	
AB(A−B)	28.86	1	28.86	18.55	0.0012	
ABC(A−B)	1.02	1	1.02	0.6588	0.4342	
Residual	17.11	11	1.56			
Lack of fit	7.45	6	1.24	0.6419	0.6994	Not significant
Pure error	9.67	5	1.93			
Cor total	665.88	18				

Table 7: Residual Strength at 718°C

Source	Sum of squares	df	Mean square	F-value	p-value	Decision
Model	521.04	7	74.43	53.0	<0.0001	Significant
Linear mixture	406.58	1	406.58	289.49	<0.0001	
AB	3.26	1	3.26	2.32	0.1557	
AC	6.95	1	6.95	4.95	0.048	
BC	14.72	1	14.72	10.48	0.0079	
ABC	0.6322	1	0.6322	0.4501	0.5161	
AB(A−B)	30.61	1	30.61	21.8	0.0007	
ABC(A−B)	0.0526	1	0.0526	0.0375	0.85	

Source	Sum of squares	df	Mean square	F-value	p-value	Decision
Residual	15.45	11	1.4			
Lack of fit	7.11	6	1.19	0.711	0.6584	Not significant
Pure error	8.34	5	1.67			
Cor total	536.49	18				

Table 8: Residual Strength at 821°C

Source	Sum of squares	df	Mean square	F-value	p-value	Decision
Model	443.31	7	63.33	52.96	<0.0001	Significant
Linear mixture	310.55	1	310.55	259.69	<0.0001	
AB	1.04	1	1.04	0.8727	0.3703	
AC	11.25	1	11.25	9.41	0.0107	
BC	15.91	1	15.91	13.3	0.0038	
ABC	1.22	1	1.22	1.02	0.335	
AB(A−B)	29.28	1	29.28	24.49	0.0004	
ABC(A−B)	0.0422	1	0.0422	0.0353	0.8544	
Residual	13.15	11	1.2			
Lack of fit	5.9	6	0.9837	0.6783	0.6776	Not significant
Pure error	7.25	5	1.45			
Cor total	456.46	18				

ANOVA and Model Adequacy

Table 9: Summary of Model Adequacy Statistics

Response	Model F	Model p	R^2	Adj. R^2	Pred. R^2	AP	SD	CV %	LOF p
Water absorption	165.66	<0.0001	0.9906	0.9846	0.9569	37.35	0.0838	2.18	0.0561
Sulphate resistance	52.14	<0.0001	0.9707	0.9521	0.9329	24.42	0.1933	2.16	0.1794
Compressive strength, 20°C	59.58	<0.0001	0.9743	0.9579	0.9292	24.26	1.25	4.87	0.6994
Residual strength, 718°C	53.00	<0.0001	0.9712	0.9529	0.9205	22.39	1.19	5.16	0.6584
Residual strength, 821°C	52.96	<0.0001	0.9712	0.9528	0.9182	23.15	1.09	5.22	0.6776

All five models were significant at $p < 0.0001$. R^2 values of 0.9707–0.9906 indicate that the models explain a large proportion of the variation represented in the available 28-day dataset. The differences between adjusted and predicted R^2 were small (0.0192–0.0346), supporting consistency between fit and internal prediction, but these differences are not treated as proof that overfitting is absent.

Lack-of-fit tests were nonsignificant for all responses ($p = 0.0561–0.6994$), indicating no statistically detectable lack-of-fit relative to the pure-error component in the repeated design points. The term-level ANOVA also shows that not every interaction was significant. For water absorption, AB and BC were significant whereas AC and ABC(A−B) were not. For sulphate resistance, AB, AC, BC, ABC and AB(A−B) were significant. For ambient and thermal strength, the dominant linear mixture effect and selected RHF-related interactions were significant, while several higher-order terms were not. Full ANOVA results are provided in Supplementary Table S1.

Fitted Regression Equations

Water Absorption

WA = −1.53225A + 0.036213B + 0.029397AB − 0.642508AC + 0.001520BC + 0.011086ABC + 0.000161AB(A−B) + 0.000049ABC(A−B)

Sulphate Resistance

SR = 0.503595A + 0.088084B − 0.004822AB − 1.78288AC + 0.003389BC + 0.030737ABC + 0.000018AB(A−B) + 0.000130ABC(A−B)

Compressive Strength at 20°C

Fc20 = 15.98570A + 0.343629B − 0.286303AB − 3.56057AC − 0.034397BC + 0.064119ABC − 0.001405AB(A−B) + 0.000326ABC(A−B)

Residual Strength at 718°C

TR718 = 13.52379A + 0.305094B − 0.242045AB − 0.694092AC − 0.026992BC + 0.012885ABC − 0.001185AB(A−B) + 0.000074ABC(A−B)

Residual Strength at 821°C

TR821 = 13.24061A + 0.280157B − 0.236084AB − 0.545540AC − 0.028061BC + 0.010249ABC − 0.001153AB(A−B) + 0.000066ABC(A−B)

These equations are empirical and should be used only within the investigated WCTP, PLC and RHF domain. The constrained mixture structure should be retained when using them, and extrapolation beyond the experimental region is not justified.

Water Absorption Response Surface

The fitted surface shows the strongest change along the WCTP–PLC axis. The predicted response ranged from about 2.67% to 4.83%, with the lowest values concentrated around moderate WCTP replacement. The experimental data show the same broad pattern: 7% WCTP without RHF gave 2.67%, whereas 30% WCTP with 2% RHF gave 4.83%. The increase at high replacement may reflect reduced cementitious binding and altered pore connectivity, while RHF provides a secondary influence through its water affinity and possible void formation. These are plausible interpretations rather than direct measurements of pore structure.

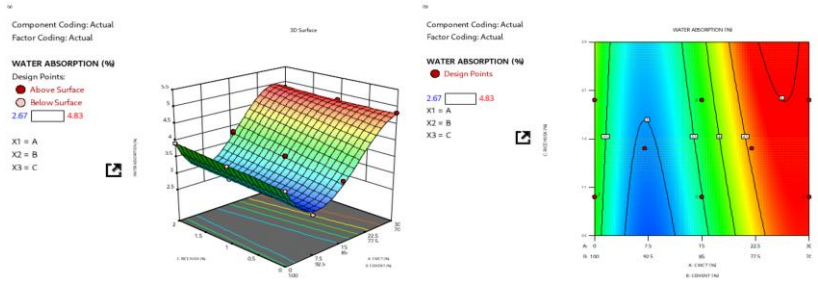


Figure 1: Response Surface and Contour Representation of Water Absorption at 28 Days

Sulphate Resistance Response Surface

Figure 2 presents the sulphate-resistance response, expressed as the compressive-strength response after sulphate exposure. Values ranged from 6.90 to 10.33 N/mm^2. The surface confirms strong interaction between binder composition and RHF, consistent with the significant AB, AC, BC and ABC terms. The response increased toward regions containing higher WCTP and RHF, although these same regions did not provide the best ambient or thermal strength. The result illustrates the trade-off that the desirability optimization was intended to resolve.

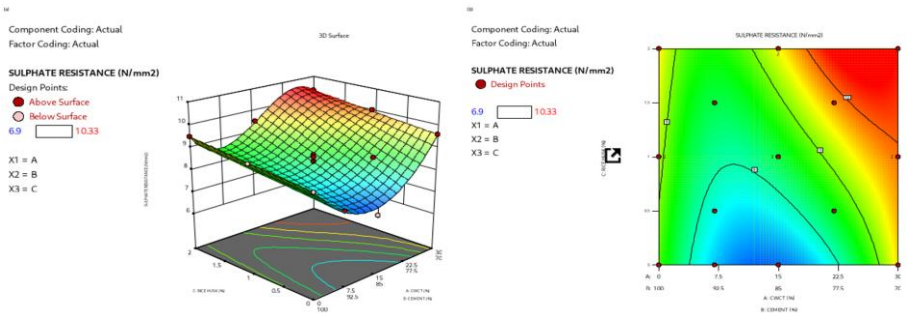


Figure 2: Response Surface and Contour Representation of Sulphate Resistance at 28 Days

Ambient Compressive Strength Response Surface

The higher-strength region is concentrated around low-to-moderate WCTP replacement and low RHF dosage. The measured 28-day strength reached 36.0 N/mm^2 at 7% WCTP without RHF, but fell to 16.0 N/mm2 at 30% WCTP with 2% RHF. Moderate ceramic replacement may benefit packing and secondary hydration, whereas excessive replacement reduces the amount of primary cementitious material. Increasing RHF can also affect workability and matrix continuity. Because porosity and fibre dispersion were not quantified for every formulation, these mechanisms remain tentative.

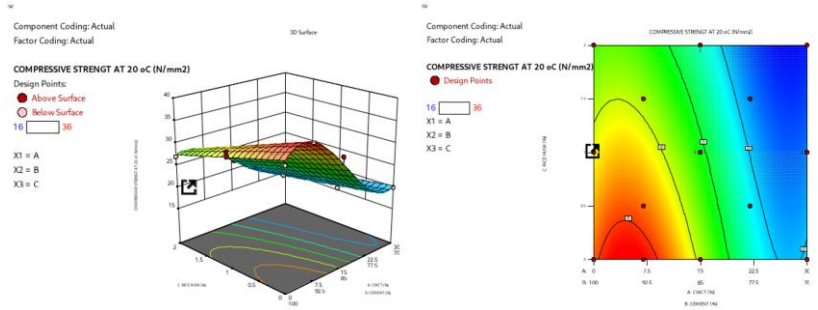


Figure 3: Response Surface and Contour Representation of Compressive Strength at 20°C at 28 Days

Residual Compressive Strength at 718°C

The predicted residual strength at 718°C ranged from approximately 14.2 to 31.7 N/mm^2. Higher values were concentrated around low-to-moderate WCTP and low RHF contents. The 7% WCTP–0% RHF formulation recorded 31.7 N/mm^2 at 28 days. Moderate ceramic replacement may help preserve matrix continuity before heating, while excessive RHF is associated with lower residual strength. The RSM results do not, however, isolate the contributions of pore evolution, fibre degradation or phase transformation.

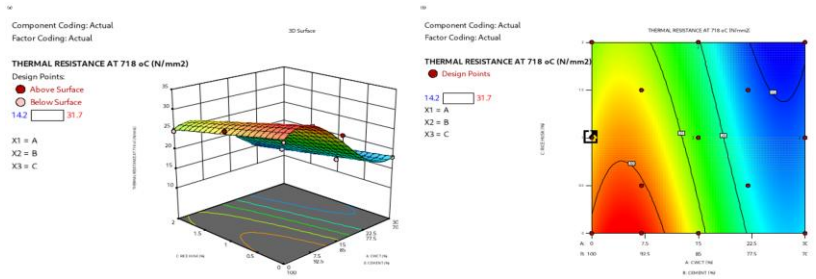


Figure 4: Response Surface and Contour Representation of Residual Compressive Strength After 718°C Exposure

Residual Compressive Strength at 821°C

The response at 821°C ranged from about 13.5 to 29.5 N/mm2. The 7% WCTP–0% RHF mixture reached 29.5 N/mm^2, N/mm2red with 27.6 N/mm^2 for the control. At high WCTP and RHF contents, residual strength declined. The trend is consistent with reduced binder availability and thermal degradation of the lignocellulosic component, but these mechanisms should be viewed as plausible explanations rather than direct causal evidence from the RSM dataset.

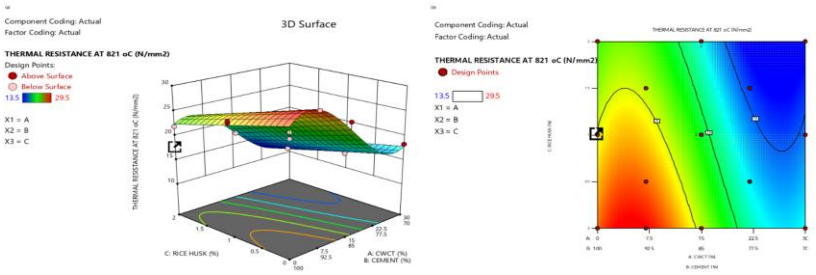


Figure 5: Response Surface and Contour Representation of Residual Compressive Strength After 821°C Exposure.

Diagnostic Assessment and Influential Observations

The diagnostic plots were examined for normality of residuals, agreement between predicted and observed values, and systematic patterns in residual-versus-predicted plots. The normal probability plots were broadly linear, while residuals were scattered around the zero reference without a pronounced funnel pattern. Predicted-versus-actual plots also showed close alignment with the equality line. These diagnostics support model adequacy, but they are not treated as proof that overfitting or influence is absent.

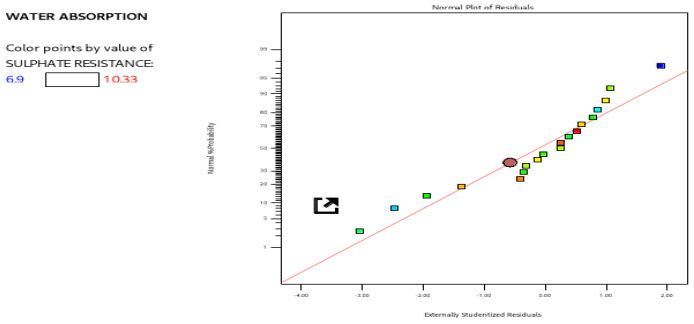


Figure 6: Diagnostic Plots for Water Absorption

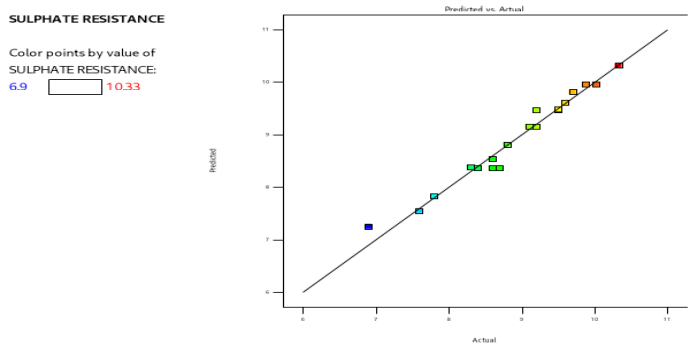


Figure 7: Diagnostic Plots for Sulphate Resistance

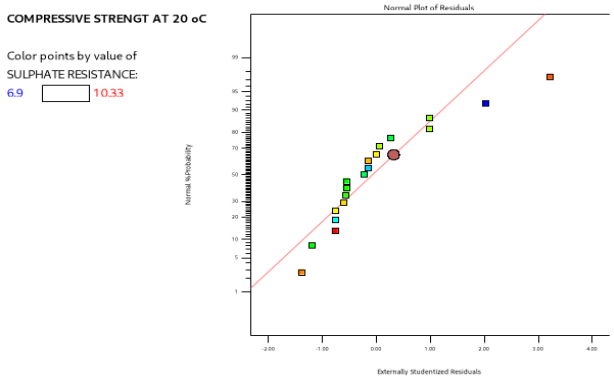


Figure 8: Diagnostic Plots for Compressive Strength at 20°C.

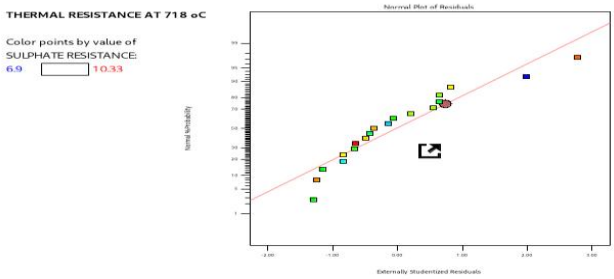


Figure 9: Diagnostic Plots for Residual Compressive Strength at 718°C

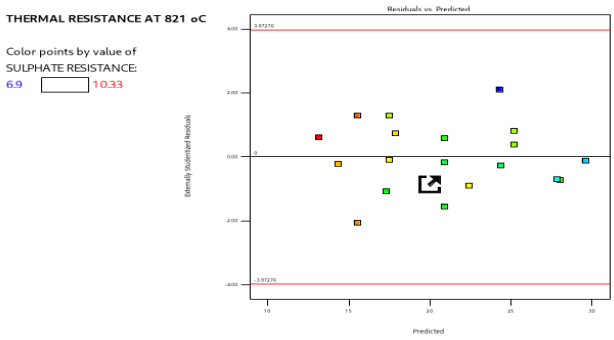


Figure 10: Diagnostic Plots for Residual Compressive Strength at 821°C

Numerical Optimization

Table 5: Optimization Criteria and Response Constraints

Factor/response	Goal	Range
WCTP	In range	0–30%
PLC	In range	70–100%
RHF	Minimize	0–2% v/v
Water absorption	Minimize	2.67–4.83%
Sulphate resistance	Maximize	6.90–10.33 N/mm^2
Compressive strength, 20°C	Maximize	16–36 N/mm^2
Residual strength, 718°C	Maximize	14.2–31.7 N/mm^2
Residual strength, 821°C	Maximize	13.5–29.5 N/mm^2

Numerical optimization identified 10.5% WCTP, 89.5% PLC and 0.03% RHF by concrete volume (approximately 0.31 kg/m³ RHF), with an overall desirability of 0.745. The predicted responses were 2.85% water absorption, 7.29 N/mm^2 sulphate resistance, 33.71 N/mm^2 ambient compressive strength, 29.72 N/mm^2 residual strength at 718°C and 27.72 N/mm^2 at 821°C.

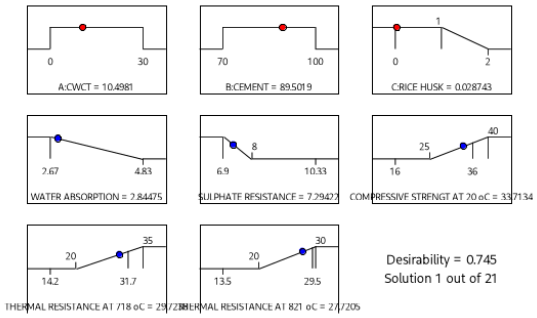


Figure 11: Optimization Ramp Showing Selected Factor Levels and Predicted Responses

The optimum should not be interpreted as the formulation giving the maximum value for every response. The 7% WCTP–93% PLC–0% RHF mixture gave the highest 28-day ambient strength (36.0 N/mm^2), whereas the numerical optimum shifted toward 10.5% WCTP and a very small RHF dosage because several responses were optimized simultaneously.

Experimental Validation and Error Assessment

Table 10: Experimental Validation of the Optimized Formulation

Response	Predicted	Observed	Absolute error	RPE (%)	Direction
Water absorption	2.85	2.72	0.13	4.78	Overprediction
Sulphate resistance	7.29	7.00	0.29	4.14	Overprediction
Compressive strength, 20°C	33.71	32.18	1.53	4.75	Overprediction
Residual strength, 718°C	29.72	28.35	1.37	4.83	Overprediction
Residual strength, 821°C	27.72	26.56	1.16	4.37	Overprediction

All five responses were slightly overpredicted at the optimum. Relative prediction errors ranged from 4.14% to 4.83%, below the 5% criterion used in the project analysis. The consistent direction of the error indicates a small positive bias at the optimum rather than purely random deviation. Because validation was performed at only one independent composition, these results provide evidence of local agreement and should not be treated as proof of generalization across the full design space.

The measured ambient compressive strength of the optimized mixture was 32.18 N/mm^2. Relative to the 34.0 N/mm^2 control at 28 days, this represents a reduction of approximately 5.4%. The optimum was therefore not a maximum-strength formulation; it represents a compromise across the competing responses.

The pooled MAE (0.896) and RMSE (1.064) from the earlier manuscript were removed because they combined responses expressed in different units and were based on a single validation composition. For one observation per response, the response-specific absolute error is numerically equivalent to both MAE and RMSE. Reporting absolute error and RPE separately provides a clearer validation assessment.

Integrated Interpretation

Taken together, the response surfaces and validation results show that WCTP was the dominant variable governing the broad mechanical and durability trends, while RHF acted mainly as a secondary modifier whose influence depended on binder composition. Moderate WCTP contents generally produced the most favourable balance for ambient and thermal strength, whereas higher RHF levels tended to reduce strength and increase water absorption. The optimized 10.5% WCTP–89.5% PLC–0.03% RHF formulation therefore represents a compromise rather than an absolute maximum for any single response.

Mechanistic explanations are deliberately cautious. The project work includes SEM observations for selected mixtures, but the RSM manuscript does not provide a complete microstructural dataset for every formulation. Explanations involving pore refinement, cement dilution, fibre-induced voids, thermal degradation or changes in hydration products are therefore presented as plausible interpretations consistent with the observed trends, not as mechanisms directly demonstrated for every response.

CONCLUSION

The study demonstrates that WCTP–RHF concrete can be represented by statistically significant RSM models within the investigated design domain. At 28 days, water absorption ranged from 2.67–4.83%, the sulphate-resistance response from 6.90–10.33 N/mm^2, ambient compressive strength from 16.0–36.0 N/mm^2, residual strength after 718°C exposure from 14.2–31.7 N/mm^2, and residual strength after 821°C exposure from 13.5–29.5 N/mm^2. The retained Cubic × Linear Scheffé models were significant at $p < 0.0001$, with R^2 values of 0.9707–0.9906 and nonsignificant lack-of-fit tests. Numerical optimization identified 10.5% WCTP, 89.5% PLC and 0.03% RHF by volume (approximately 0.31 kg/m^3 RHF), with an overall desirability of 0.745. Experimental validation produced relative prediction errors of 4.14–4.83%, although all five responses were slightly overpredicted. The optimized mixture recorded 32.18 N/mm^2 at ambient temperature, about 5.4% below the 34.0 N/mm^2 control, confirming that the optimum was a multi-response compromise rather than the maximum-strength mixture. The models should therefore be used for prediction only within the tested composition ranges and should be supported by additional independent validation before broader practical mix-design decisions are made.

REFERENCES

Adamu, M., Mohammed, B. S., & Liew, M. S. (2022). Optimization of concrete mix using response surface methodology. Case Studies in Construction Materials, 16, e00905.

ASTM International. (2021). ASTM C642-21: Standard test method for density, absorption, and voids in hardened concrete. ASTM International.

ASTM International. (2022). ASTM C150/C150M-22: Standard specification for Portland cement. ASTM International.

ASTM International. (2023). ASTM C33/C33M-23: Standard specification for concrete aggregates. ASTM International.

ASTM International. (2023). ASTM C618-23: Standard specification for coal fly ash and raw or calcined natural pozzolan for use in concrete. ASTM International.

Bisht, K., & Ramana, P. V. (2020). Sustainable production of concrete containing discarded rice husk fibers. Construction and Building Materials, 264, 120270. https://doi.org/10.1016/j.conbuildmat.2020.120270

British Standards Institution. (2019). BS EN 12390-3: Testing hardened concrete—Part 3: Compressive strength of test specimens. BSI.

Chen, Y., Zhang, P., Sha, D., & Wang, J. (2021). Effect of rice husk fiber on fresh and hardened properties of sustainable concrete composites. Materials, 14(11), 2945. https://doi.org/10.3390/ma14112945

Council for the Regulation of Engineering in Nigeria. (2017). Nigerian code of practice for structural concrete. COREN.

Design-Expert Software, Stat-Ease Inc. (2023). Design-Expert® software version 13 user guide. Stat-Ease Inc.

Hadee, A., & Shakeel, M. (2022). Optimization of ceramic powder concrete using response surface methodology. Materials Today: Proceedings, 62, 5200–5207.

International Energy Agency. (2023). Technology roadmap: Low-carbon transition in the cement industry. IEA Publications.

International Organization for Standardization. (1999). ISO 834-1: Fire-resistance tests—Elements of building construction—Part 1: General requirements. ISO.

Khoury, G. A. (2019). Behaviour of concrete at high temperatures. In Advanced concrete technology (pp. 1–34). Elsevier.

Kumar, S., & Bhattacharyya, S. (2021). Interfacial behaviour of lignocellulosic fibers in cementitious composites. Journal of Cleaner Production, 294, 126305.

Medina, C., Sánchez de Rojas, M. I., & Frías, M. (2013). Reuse of sanitary ceramic wastes as supplementary cementitious materials in eco-efficient concretes. Cement and Concrete Composites, 34(1), 48–54.

Mehta, P. K., & Monteiro, P. J. M. (2014). Concrete: Microstructure, properties, and materials (4th ed.). McGraw-Hill Education.

Miller, S. A., Horvath, A., & Monteiro, P. J. M. (2024). Readily implementable techniques can cut annual CO_2 emissions from the production of concrete by over 20%. Nature Sustainability, 7(1), 1–10.

Montgomery, D. C. (2019). Design and analysis of experiments (10th ed.). John Wiley & Sons.

Myers, R. H., Montgomery, D. C., & Anderson-Cook, C. M. (2016). Response surface methodology: Process and product optimization using designed experiments (4th ed.). John Wiley & Sons.

Onuaguluchi, O., & Banthia, N. (2022). Natural fibres in cement composites. Cement and Concrete Research, 158, 106874.

Pacheco-Torgal, F., & Jalali, S. (2011). Compressive strength and durability properties of ceramic waste-based concrete. Construction and Building Materials, 25(2), 898–905.

Phan, L. T., & Carino, N. J. (2001). Fire performance of high-strength concrete: A report of the state-of-the-art. National Institute of Standards and Technology.

Scheffé, H. (1958). Experiments with mixtures. Journal of the Royal Statistical Society: Series B (Methodological), 20(2), 344–360.

Scrivener, K. L., John, V. M., & Gartner, E. M. (2018). Eco-efficient cements: Potential economically viable solutions for a low-CO_2 cement-based materials industry. Cement and Concrete Research, 114, 2–26.

Siddique, R., Kaur, G., & Singh, M. (2023). Utilization of waste ceramic powder in concrete: A review. Construction and Building Materials, 380, 131221.

Singh, M., & Siddique, R. (2017). Effect of waste ceramic tile powder on properties of concrete. Resources, Conservation and Recycling, 123, 48–57. https://doi.org/10.1016/j.resconrec.2017.03.002

Tayeh, B. A., Almeshal, I., Alyousef, R., Alabduljabbar, H., & Mohamed, A. M. (2021). Durability and mechanical performance of hybrid waste ceramic and agricultural fiber concrete. Journal of Building Engineering, 43, 102880. https://doi.org/10.1016/j.jobe.2021.102880

Yuzer, N., Akbulut, H., & Yildirim, Y. (2021). Thermal degradation of natural fibers in cement composites. Journal of Building Engineering, 35, 101974.

©2026 This is an Open Access article distributed under the terms of the Creative Commons Attribution 4.0 International license viewed via https://creativecommons.org/licenses/by/4.0/ which permits unrestricted use, distribution, and reproduction in any medium, provided the original work is cited appropriately.